

## Chapter 5 Spacecraft Environmental Conditions

### Table of Contents

5	Spacecraft Environmental Conditions .....	5-1
5.1	Mechanical Environment .....	5-1
5.1.1	General .....	5-1
5.1.2	Quasi-Static Accelerations.....	5-2
5.1.3	Low Frequency Vibration .....	5-3
5.1.4	Acoustic Noise .....	5-4
5.1.5	Random Vibration .....	5-5
5.1.6	Shock.....	5-5
5.1.7	Loads during Ground Operations .....	5-7
5.1.7.1	Handling Loads During Ground Operations .....	5-8
5.1.7.2	Spacecraft Container Railway Transportation Loads .....	5-8
5.1.7.3	Roadway Autonomous Transportation in Archangel and Plesetsk Cosmodrome .....	5-9
5.1.7.4	Loads during Transport in Upper Composite.....	5-10
5.2	Thermal Environment .....	5-11
5.2.1	Environmental Conditions in the Integration Facility .....	5-11
5.2.2	Pre-Launch Temperature Control within the Fairing .....	5-11
5.2.3	In-flight Temperature under the Fairing .....	5-13
5.2.4	Aerothermal Flux at Fairing Jettisoning .....	5-14
5.2.5	Heat Impact during Coasting Phase .....	5-14
5.3	Fairing Static Pressure during the Ascent .....	5-14
5.4	Contamination and Cleanliness.....	5-15
5.5	Electromagnetic Environment .....	5-15
5.5.1	Launch Vehicle Electro-Magnetic Emissions .....	5-15
5.5.2	Spacecraft Electro-Magnetic Emissions .....	5-17

## List of Figures

Figure 5-1	Launch vehicle and payload coordinate system.....	5-1
Figure 5-2	Typical axial payload interface acceleration.....	5-2
Figure 5-3	Typical radial payload interface acceleration. ....	5-3
Figure 5-4	Low frequency vibration environment at the separation plane. ....	5-4
Figure 5-5	Composite noise spectrum under the <i>Rockot</i> payload fairing during flight given in 1/3 octave band referenced to $2 \times 10^{-5}$ Pa RMS. ....	5-4
Figure 5-6	Typical shock environment for diverse separation systems. ....	5-6
Figure 5-7	Transportation of the spacecraft in the spacecraft container. ....	5-7
Figure 5-8	Spacecraft transportation as part of the upper composite.....	5-7
Figure 5-9	Random vibration power spectrum acting at spacecraft container base during autonomous railway transportation. ....	5-8
Figure 5-10	Random vibration spectrum for autonomous roadway transportation.....	9
Figure 5-11	Random vibration power spectrum acting on the spacecraft during upper composite transportation.....	10
Figure 5-12	Thermal conditioning of the upper composite during transportation. ....	5-12
Figure 5-13	Thermal conditioning of the upper composite at the launch pad.....	5-12
Figure 5-14	Variation of fairing inner static pressure during ascent. ....	5-15
Figure 5-15	Field strength of launch vehicle and cosmodrome electromagnetic emissions in the adapter plane without payload fairing.....	5-16
Figure 5-16	Allowable spacecraft emissions at Plesetsk Cosmodrome. ....	5-17

## List of Tables

Table 5-1	Quasi-static loads experienced by an average payload during ascent. ....	5-3
Table 5-2	Low frequency vibration environment.....	5-3
Table 5-3	Composite noise spectrum under the fairing during flight. ....	5-5
Table 5-4	Typical shock environment for diverse separation systems. ....	5-6
Table 5-5	Maximum handling loads.....	5-8
Table 5-6	Shock loads during autonomous railway transportation.....	5-8
Table 5-7	Random vibration power spectrum acting at spacecraft container base during autonomous railway transportation. ....	5-8
Table 5-8	Quasi-static accelerations for autonomous roadway transportation at wind velocities $\leq 20$ m/s. ....	5-9
Table 5-9	Random vibration power spectrum for autonomous roadway transportation. ....	5-9
Table 5-10	Accelerations during upper composite transportation at wind velocities $\leq 20$ m/s.....	5-10
Table 5-11	Random vibration power spectrum acting on the spacecraft during upper composite transportation.....	5-10
Table 5-12	Air conditioning systems performance data. ....	5-13
Table 5-13	Ranges of measured parameters under the payload fairing. ....	5-13
Table 5-14	Launch vehicle and cosmodrome electromagnetic emissions. ....	5-16
Table 5-15	Allowable spacecraft emissions at Plesetsk Cosmodrome. ....	5-17

# 5 Spacecraft Environmental Conditions

This section describes the environment to which the spacecraft is exposed during the launch site operations and its transport into orbit with the *Rocket* launcher as well as accelerations occurring during ground transportation and handling.

## 5.1 Mechanical Environment

### 5.1.1 General

During flight, the payload is subjected to static and dynamic loads induced by the launch vehicle. Such excitation may be of aerodynamic origin, especially wind and gusts, buffeting in the transonic flight re-

gime, or may be due to loading induced by the operation of the propulsion systems due to longitudinal acceleration, thrust build-up or tail-off transients, structure-propulsion coupling, attitude control operation, etc.

The various types of mechanical environment experienced by the payload are described in the following paragraphs. Typical data are given for sine, random and shock environments. If not explicitly stated, all mechanical loads are defined as maximum operational loads. They are estimated with 90% confidence and their levels will not be exceeded in 99% of all flights. For different dispenser types, dedicated environments have to be defined on a case-by-case basis.

For the launch vehicle and payload coordinate system refer to Figure 5-1.

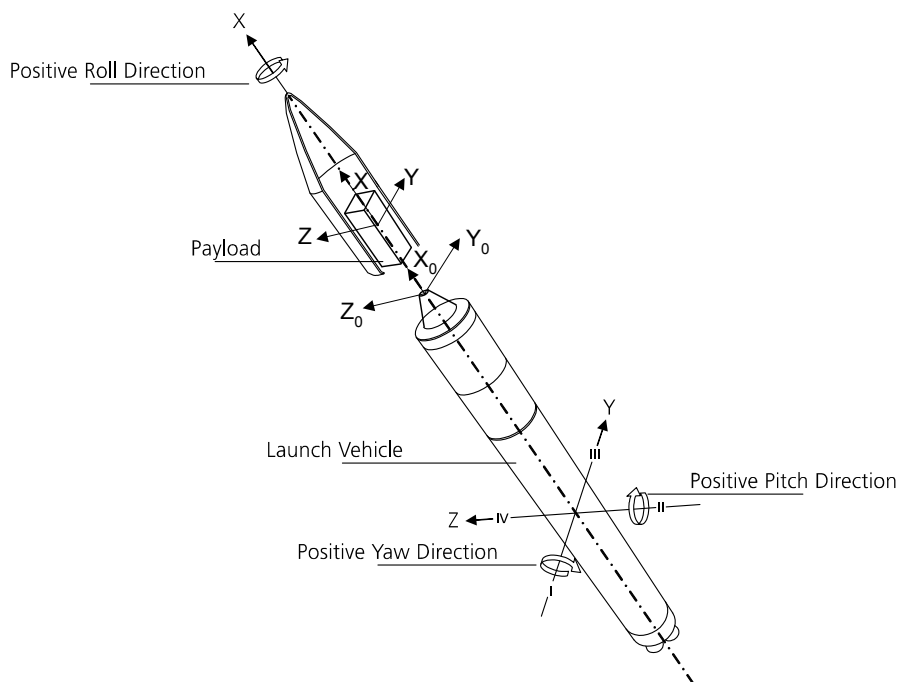


Figure 5-1 Launch vehicle and payload coordinate system.

The spacecraft coordinate system without index may be selected with the origin at the CoM of the spacecraft or in the attachment plane and with axes parallel to the launch vehicle coordinate system, if the satellite is clocked orthogonally. The orbital block coordinate system with the index "O" is a useful tool for the definition of the loads and performance of the coupled loads analysis (CLA). Its origin lies in the *Breeze-KM* / payload adapter interface plane. The Y and Z axes concur with the launch vehicle stabilisation axes III and IV respectively.

### 5.1.2 Quasi-Static Accelerations

During ascent, the payload will experience dynamic loads generated by

- the operating launch vehicle propulsion unit,
- the aerodynamic forces appearing as the launch vehicle traverses dense atmospheric layers, and
- the operating launch vehicle navigation system.

The low-frequency or quasi-static component of dynamic loading, which is the frequency component below 100 Hz is used as the dimensioning factor when selecting technical solutions aimed at ensuring adequate strengths of the payload and adapter system structures.

Figure 5-2 and Figure 5-3 show typical low-frequency spacecraft interface accelerations during powered flight of stages 1 and 2. Payload accelerations during powered flight of the upper stage are much smaller and, thus, of no concern for the structure's load capability.

Quasi-static loads experienced by the spacecraft are largely determined by the spacecraft mass and stiffness properties. The loads given in Table 5-1 can be used as preliminary dimensioning inputs to the design of the spacecraft. These loads are the worst-case limit loads that do not necessarily apply to any spacecraft. Instead, they are obtained for an average spacecraft and shall be subject to updates by a dedicated CLA for each particular mission.

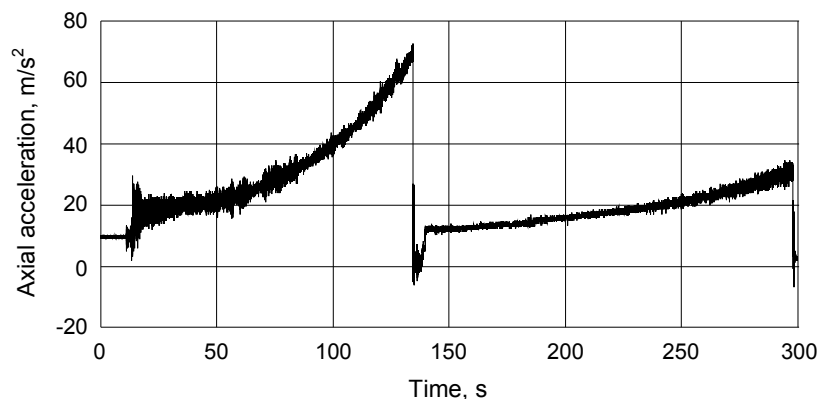


Figure 5-2 Typical axial payload interface acceleration.

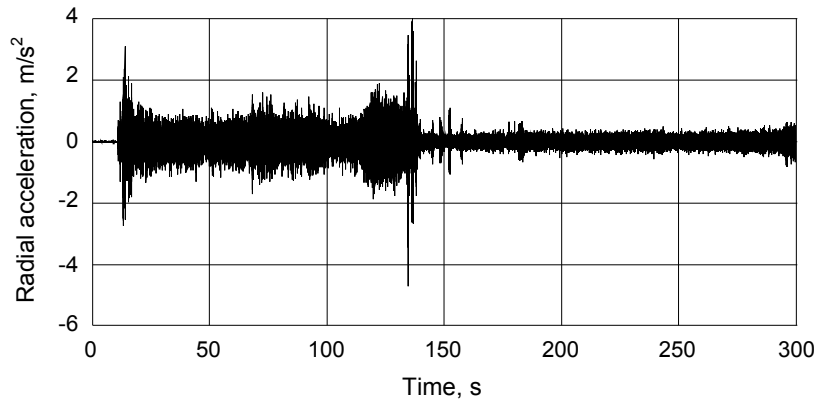


Figure 5-3 Typical radial payload interface acceleration.

Seq.	Event	axial, g		
		max	min	radial, g
1	Lift-off	+ 3.6	0	± 0.7
2	Worst-case dynamic pressure $q_{max}$	+ 2.8	+ 2.4	± 0.9
3	Peak stage 1 thrust $P_{max}$	+ 8.0	+ 6.2	± 0.5
4	Worst-case axial stage 1 structural acceleration $n_{xmax}$	+ 8.1	+ 6.3	± 0.5
5	Stage 1 shutdown	+ 8.1	- 1.5	± 0.7
6	Stage 2 powered flight	+ 3.0	0	± 0.4
7	Upper stage powered flight	+ 1.6	0	± 0.4

Note:

- 1) "+" means compression, "-" means tension
- 2) Axial and radial loads may exist simultaneously.

Table 5-1 Quasi-static loads experienced by an average payload during ascent.

### 5.1.3 Low Frequency Vibration

The low frequency longitudinal and lateral vibration environment spectra experienced at the spacecraft separation plane are presented in Table 5-2 and Figure 5-4 respectively.

Frequency, Hz	Acceleration, g	
	Longitudinal	Lateral
5 - 10	0.8	0.5
10 - 20	0.8 - 1.2	0.5
20 - 40	1.2 - 0.8	0.5
40 - 100	0.8	0.5

Table 5-2 Low frequency vibration environment.

These values are subject to revision after the performance of a CLA with a dedicated structural mathematical model of the spacecraft.

A notching to design loads can be allowed based on controller data at the adapter interface to the spacecraft or at the interface to *Breeze-KM* whichever is more critical.

For test approaches and factors please refer to chapter 6.

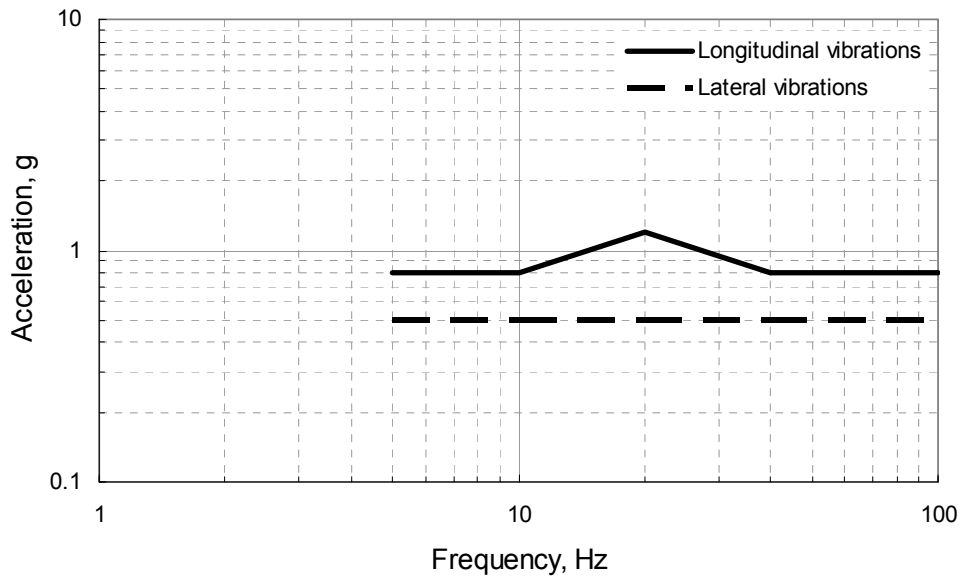


Figure 5-4 Low frequency vibration environment at the separation plane.

#### 5.1.4 Acoustic Noise

The spacecraft is exposed to an acoustic environment throughout the boost phase of flight until the vehicle is out of the atmosphere. Acoustic noise is generated by engine noise, buffeting and boundary layer noise. The level is highest at lift-off (137.9 dB OASPL) and in the transonic phase (135 dB OASPL) with a RMS reference

pressure of  $2 \times 10^{-5}$  Pa = 0 dB. Noise is substantially lower outside these periods.

The composite noise spectrum at lift-off is given in Figure 5-5 and Table 5-3. The given spectra reflect the guaranteed upper limit, including the worst case fill factor for spacecraft within the payload fairing. The composite duration is 10 seconds.

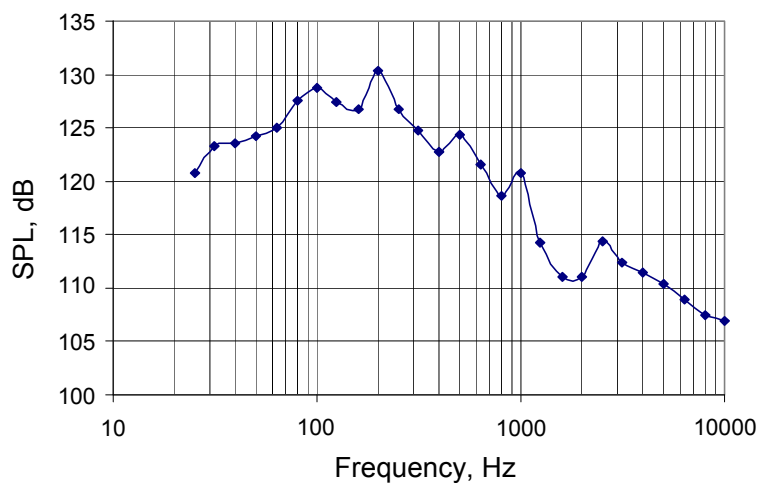


Figure 5-5 Composite noise spectrum under the *Rockot* payload fairing during flight given in 1/3 octave band referenced to  $2 \times 10^{-5}$  Pa RMS.

1/3 octave band centre frequency, Hz	Sound pressure level, dB
25	120.7
31.5	123.3
40	123.5
50	124.2
63.5	125.0
80	127.4
100	128.7
125	127.4
160	126.8
200	130.4
250	126.7
315	124.7
400	122.8
500	124.4
630	121.5
800	118.6
1000	120.7
1250	114.3
1600	111.1
2000	111.1
2500	114.4
3150	112.4
4000	111.4
5000	110.4
6300	108.9
8000	107.4
10000	106.9
OASPL	137.9

Note:

- The acoustic loads are referenced to the RMS acoustic pressure of  $2 \times 10^{-5}$  Pa
- Test duration and factors are defined in chapter 6
- Composite duration is 10 seconds

**Table 5-3 Composite noise spectrum under the fairing during flight.**

### 5.1.5 Random Vibration

Random vibration is mainly generated by the acoustic noise field under the payload fairing and is also transmitted via the launcher structure. Random accelerations excited by the launch vehicle engines can be neglected for spacecraft design. The

random vibration depends on specific payload configuration, e.g. fill factor, payload adapter, payload surfaces. Therefore a generic random vibration environment is not defined here. In the case of small compact satellites it may be more convenient to perform a random vibration test. In this particular case, the customer is asked to contact EUROCKOT directly for definition of the appropriate random vibration test levels.

### 5.1.6 Shock

The spacecraft is subjected to a shock environment during separation of the fairing and launch vehicle components as well as spacecraft separation.

The shock levels at the spacecraft separation plane experienced during the separation from the *Breeze-KM* upper stage are associated with the separation system selected (section 4.2).

The shock levels are also dependent on the pre-tension of the bolts for the MLS system or the pre-tension of the band for the clamp band systems. Pre-tensions are determined according to the spacecraft and interface characteristics such as spacecraft CoM and interface diameter in relation to the separation system following qualified standards. Table 5-4 and Figure 5-6 show the shock specifications for the fairing separation as well as the MLS and EADS CASA clamp band systems with typical pre-tensions.

For detailed information for other sizes, special pre-tensions and low shock systems, please contact EUROCKOT.

Shock loads are defined as worst value applicable to all three axes and they act

simultaneously. For clamp band systems the shock loads are measured in radial, tangential directions to the clamp band and normal to the separation plane. Please

note that the second stage separation shock levels are lower than the specifications given here, thus not to be considered in the shock environment.

Frequency, Hz	Acceleration, g (SRS, Q=10)				
	Fairing Separation**	Mechanical Lock System*	CASA CRSS 937 SRF*	CASA CRSS 1194	Small satellite separation system
100	50	50	80	80	40
700	700	800	1000	1000	400
1000	1000	2000	1800	1800	600
1500	1000	2000	2800	2800	
2000	1000		2800	2800	1500
4000	1000	4000	2800	2800	
5000	1000	4000			
6000	1000				1800
10000	1000	2000			1800

\* Shock values for separation systems are measured 40 mm above the separation plane.

\*\* Fairing separation shock is defined at the base of the payload adapter. Hence, for taller payload adapters shock at the spacecraft to adapter interface plane will be lower.

**Table 5-4 Typical shock environment for diverse separation systems.**

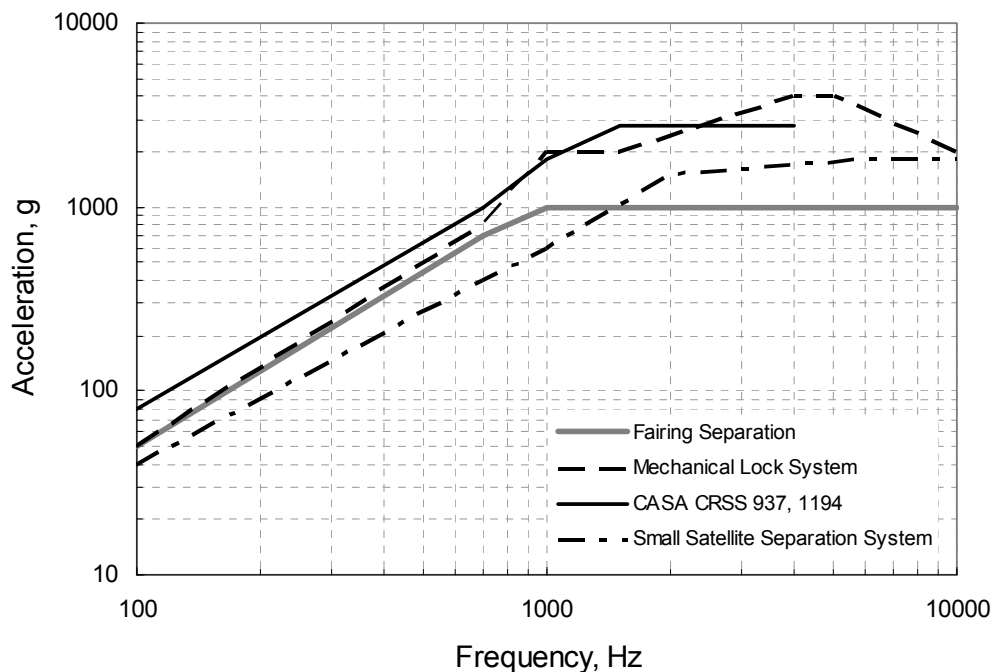


**Figure 5-6 Typical shock environment for diverse separation systems.**



### 5.1.7 Loads during Ground Operations

This section presents the ground loads the spacecraft or its container is subjected to on the EUROCKOT standard ground transportation route from the port-of-entry Archangel Talagi Airport to Plesetsk Cosmodrome by lorry and railway. The right-handed co-ordinate systems used for the different ground operations are defined in Figure 5-7 and Figure 5-8. All loads that are specified in this section are 3 sigma values with 90% confidence. The accelerations during the transportation are defined for wind velocities less than 20 m/s.

Section 5.1.7.1 provides the maximum handling loads to be expected on the

spacecraft container. Section 5.1.7.2 contains the loads given for spacecraft container transportation with a railway wagon as per the co-ordinate definitions in Figure 5-7. Similarly, section 5.1.7.3 provides loads for short duration truck transport from the Archangel airport to the railhead in Plesetsk and within the Cosmodrome, if applicable. Finally, section 5.1.7.4 provides the loads on the spacecraft during railway transportation to the launch pad as part of the *Rockot* launch vehicle upper composite. The specific measurement plan and positions of the instrumentation (Figure 5-7, Figure 5-8) can be customised for each customer's individual project.

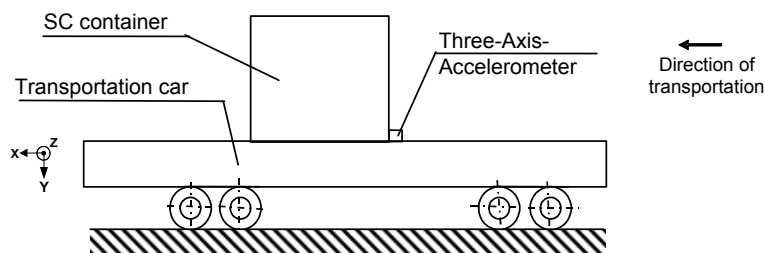


Figure 5-7 Transportation of the spacecraft in the spacecraft container.

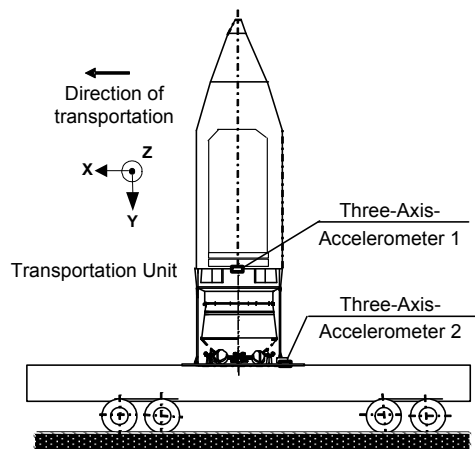


Figure 5-8 Spacecraft transportation as part of the upper composite.

### 5.1.7.1 Handling Loads During Ground Operations

The maximum handling loads acting at the spacecraft CoM during the ground operations, e. g. hoisting, are presented in Table 5-5. While the gravity acceleration acts continuously in the vertical direction, other operational loads may act simultaneously along the other directions.

Quasi-static loads		Safety factor
Vertical direction	Lateral directions	
1±0.5	±0.3	1.5

Table 5-5 Maximum handling loads.

### 5.1.7.2 Spacecraft Container Railway Transportation Loads

The location of the accelerometers and the co-ordinate system for the load measurement during the spacecraft container transport by railway are defined in Figure 5-7. The loads for railway transportation from Archangel to Plesetsk are defined in Table 5-6, Table 5-7 and Figure 5-9.

Direction	Amplitude, g	Impulse duration, s	Number of loads
X	1.0	0.16 - 0.035	100
Y	1.0		
Z	0.5		

Note: The impulse form can either be a triangle or half-sine.

Table 5-6 Shock loads during autonomous railway transportation.

Frequency, Hz	Power spectral density, g <sup>2</sup> /Hz direction		
	X	Y	Z
2	1.5E-4	7.5E-4	6.0E-4
4	8.0E-4	1.0E-2	8.0E-4
8	3.0E-3	1.0E-2	1.0E-3
10	1.0E-3	1.0E-2	3.0E-3
14	8.0E-4	3.0E-3	1.0E-3
20	8.0E-4	1.0E-3	1.0E-3
25	8.0E-4	8.0E-4	1.0E-3
30	8.0E-4	1.5E-3	1.0E-3
35	1.2E-3	8.0E-4	1.0E-3
40	4.0E-4	6.0E-4	1.5E-4
45	4.0E-4	4.3E-4	1.5E-4
50	4.0E-4	2.8E-4	1.5E-4
Time, min	420	420	420

Table 5-7 Random vibration power spectrum acting at spacecraft container base during autonomous railway transportation.

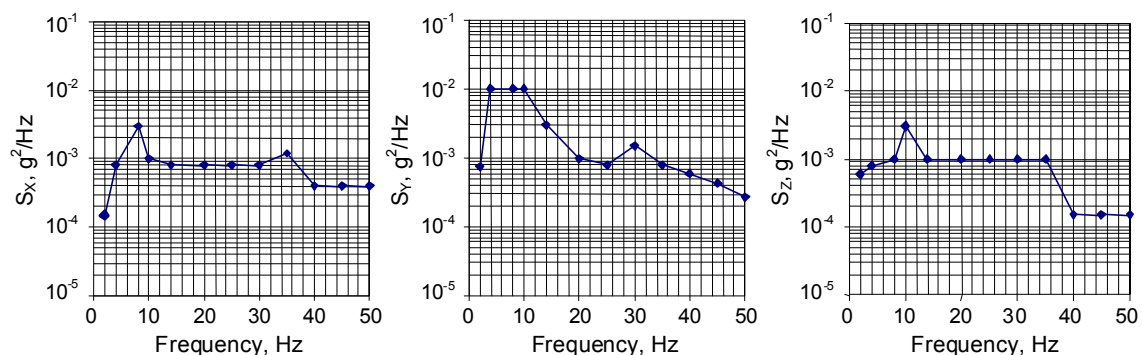


Figure 5-9 Random vibration power spectrum acting at spacecraft container base during autonomous railway transportation.

### 5.1.7.3 Roadway Autonomous Transportation in Archangel and Plesetsk Cosmodrome

The quasi-static acceleration loads for the short duration roadway transportation in Archangel are defined Table 5-8, and Figure 5-10. The random vibration loads are defined in Table 5-9. These spectra apply also to the short road transportation at the launch site in the Plesetsk Cosmodrome. The reference coordinate system definition given in Figure 5-7 also applies to the roadway autonomous transportation.

Quasi-static accelerations, g			Safety factor
X	Y	Z	
±1.0	1±1.0	±0.5	1.5

Note: For transportation regimes the loads are applied according to the coordinate system of the transportation system. The loads may apply at the same time on axes X, Y and Z.

**Table 5-8** Quasi-static accelerations for autonomous roadway transportation at wind velocities ≤ 20 m/s.

Frequency, Hz	Power spectral density, g <sup>2</sup> /Hz direction		
	X	Y	Z
2	5.0E-5	7.0E-4	4.0E-4
4	1.2E-4	3.0E-3	5.5E-4
8	3.0E-4	3.0E-3	7.0E-4
10	3.0E-4	3.0E-3	7.0E-4
14	3.0E-4	3.0E-3	7.0E-4
20	1.0E-4	4.0E-4	3.0E-4
25	4.0E-5	1.5E-4	1.0E-4
30	1,3E-5	5.0E-5	4,5E-5
35	6.0E-6	2.0E-5	2.0E-5
40	3.0E-6	1.0E-5	1.0E-5
45	2.0E-6	6.0E-6	6.0E-6
50	1.0E-6	3.2E-6	3.2E-5
Time, min	10	10	10

**Table 5-9** Random vibration power spectrum for autonomous roadway transportation.

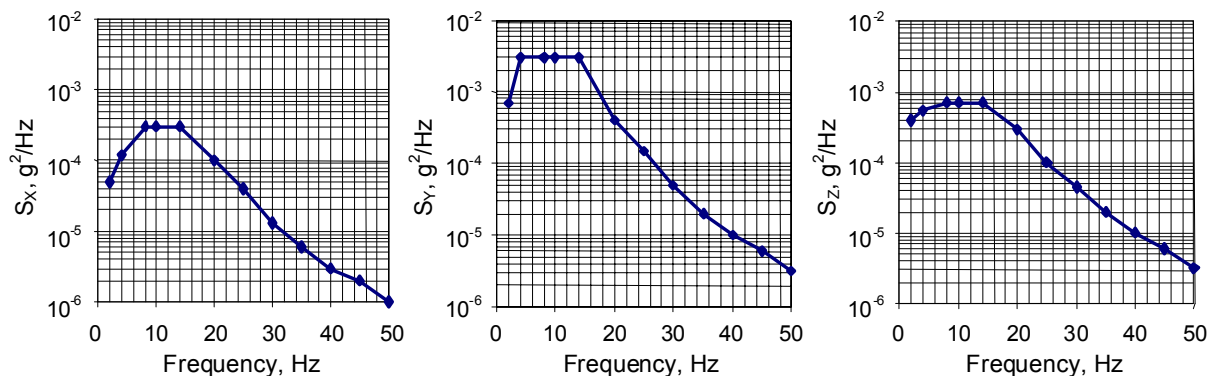


**Figure 5-10** Random vibration spectrum for autonomous roadway transportation.

### 5.1.7.4 Loads during Transport in Upper Composite

The location of the accelerometers and the co-ordinate system for spacecraft transport within the upper composite are defined in Figure 5-8. The upper composite is transported over a distance of 7 km at 3 to 5 km/h. The corresponding loads are defined in Table 5-10, Table 5-11 and Figure 5-11. The loads may act simultaneously in the respective axes.

Quasi-static accelerations ,g			Safety factor
X	Y	Z	
±1.0	1±0.5	±0.3	1.5

**Table 5-10** Accelerations during upper composite transportation at wind velocities ≤ 20 m/s.

Frequency, Hz	Power spectral density, g <sup>2</sup> /Hz direction		
	X	Y	Z
2	6.0E-5	6.0E-5	1.2E-4
4	2.0E-4	1.0E-4	1.5E-4
8	4.5E-4	5.0E-4	2.0E-4
10	1.5E-4	5.0E-4	3.0E-4
14	1.2E-4	5.0E-4	1.0E-4
20	1.2E-4	1.5E-4	1.0E-4
25	1.2E-4	1.2E-4	1.0E-4
30	1.2E-4	1.5E-4	1.0E-4
35	2.0E-4	1.1E-4	1.0E-4
40	1.5E-4	1.0E-4	3.7E-5
45	1.0E-4	8.3E-5	3.7E-5
50	1.0E-4	7.5E-5	3.7E-5
Time, min	18	18	18

**Table 5-11** Random vibration power spectrum acting on the spacecraft during upper composite transportation

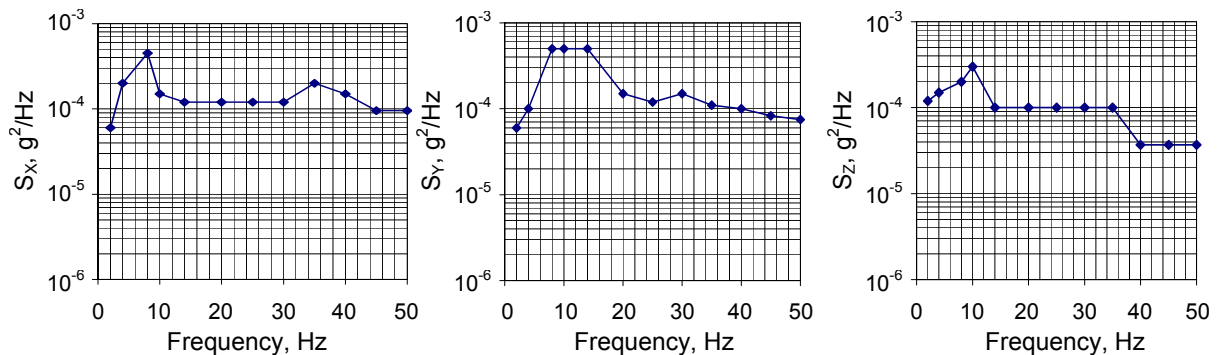


**Figure 5-11** Random vibration power spectrum acting on the spacecraft during upper composite transportation.

## 5.2 Thermal Environment

This section describes the thermal environment of the spacecraft before and after launch. For the definition of the spacecraft thermal environment, three phases of the mission are considered:

- The spacecraft preparation phase within the preparation buildings,
- transportation to the launch pad, when the spacecraft is encapsulated inside the fairing, and
- the in-flight environment phase after mating the upper composite with the launch vehicle.

### 5.2.1 Environmental Conditions in the Integration Facility

The payload is processed in clean rooms of the integration facility MIK. The clean rooms are compliant with ISO Standard 14644-1 Class 8 (former FED-STD-209 Class 100,000) with a regulated temperature of 18 to 25 °C and relative humidity between 30 and 60%. EUROCKOT can also provide ISO Class 7 cleanliness (former Class 10,000) as an optional service.

### 5.2.2 Pre-Launch Temperature Control within the Fairing

After encapsulation and upper composite integration, conditioned air to the fairing is supplied either by a mobile thermal conditioning system on a railcar or a stationary thermal conditioning system at the launch pad. A removable thermal cover is installed on the outer fairing surface for the duration of the upper composite transportation from the integration facility to the launch site, the upper composite lifting into the service tower, and the upper composite installation on the booster unit. A supplementary spacecraft battery air conditioning system can be provided as an optional service.

The upper composite air conditioning configuration during transportation from the integration facility to the launch pad and while at the launch pad is shown in Figure 5-12 and Figure 5-13.

The basic performance data of the mobile air conditioning system, the characteristics of the air supplied by the upper composite stationary air conditioning system, and the characteristics of the air supplied by the optional spacecraft battery air conditioning system are shown in Table 5-12.

The mobile and stationary air conditioning systems are compatible with ISO Class 8 cleanliness, ISO Class 7 can be provided as an optional service. The mean air velocity induced by the thermal conditioning system within the fairing does not exceed 3 m/s.

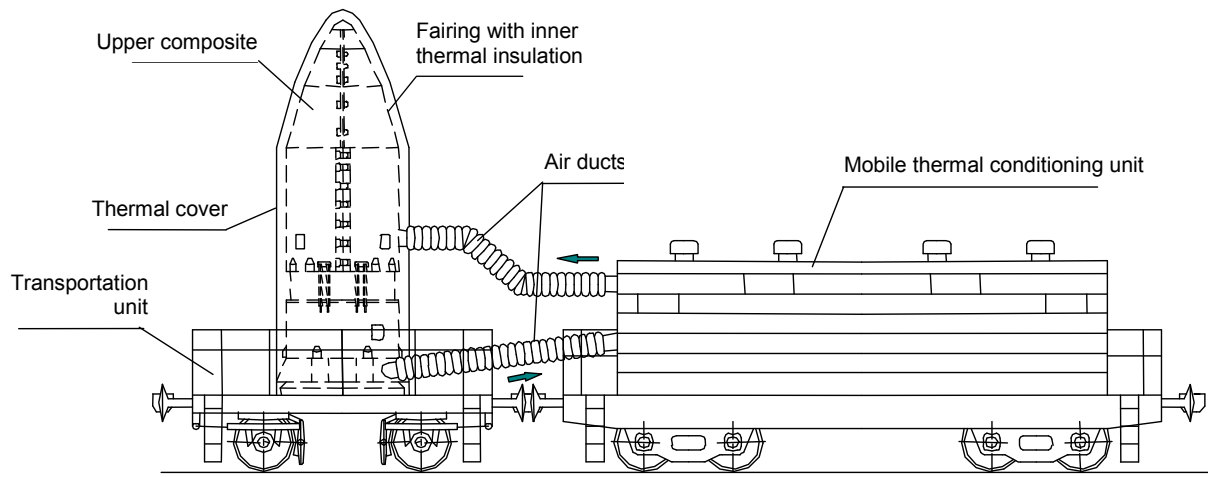


**Figure 5-12 Thermal conditioning of the upper composite during transportation.**

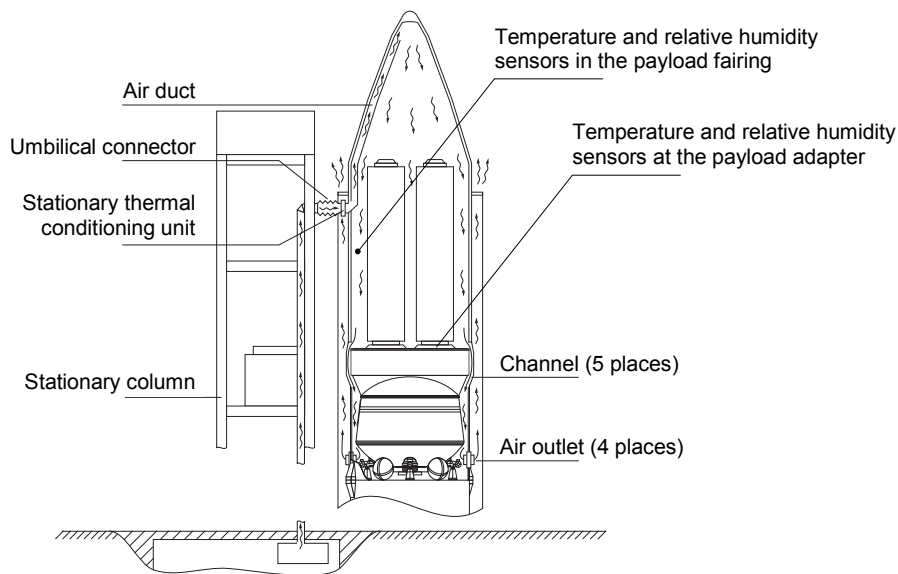


**Figure 5-13 Thermal conditioning of the upper composite at the launch pad.**

The air temperature inside the fairing is between 10 and 25°C during active temperature control, and between 5 and 30°C when no active temperature control is provided. These ranges will be updated on the basis of thermal analysis results. The thermal analysis will be performed by means of the spacecraft thermal and geo-

metric mathematical models to be provided by the Customer. The adapter hardware temperature, fairing inside air temperature and humidity will be measured and recorded by the ground measurement system during the upper composite transportation en route to the launch pad and during processing on the launch pad (Table 5-13).

Parameter	Mobile thermal conditioning unit	Stationary thermal conditioning unit	SC batteries system (optional service)
Temperature of supplied air, °C	10..25 (adjustable)	10..25 (adjustable)	7...20 (adjustable)
Dew point of supplied air, °C			≤ -20
Relative humidity of supplied air, %	30* - 60	≤ 30	
Air flow rate, m <sup>3</sup> /h	≥ 4,000	≥ 4,000	200
Static overpressure inside payload fairing, Pa	2,000	2,000	12,000
Cleanliness of supplied air	ISO Class 8 (ISO Class 7 optional)	ISO Class 8 (ISO Class 7 optional)	ISO Class 8

\* Optionally, a relative humidity of less than 30% can be maintained.

**Table 5-12 Air conditioning systems performance data.**

Parameter	Number of sensors	Measurement range	Measurement accuracy
Fairing internal air temperature within approx. 3 m of fairing separation plane	2	- 40 ... 80°C	± 0.7°C
Fairing internal air humidity within approx. 3 m of fairing separation plane	2	5 ... 90 %	± 3 %
Adapter hardware temperature at 1/2 adapter height	2	- 40... 80°C	± 0.7°C

**Table 5-13 Ranges of measured parameters under the payload fairing.**

Air conditioning of the upper composite is provided up to approximately 30 seconds before lift-off and is restarted in about 1 minute in case of a launch abort. The total number of thermal conditioning interruptions is four:

- Upper composite lifting into the service tower
- Upper composite installation on the booster unit
- Stiffness ring removal
- Installation of LTC extension

The duration of each interruption period does not exceed 1 hour. In these periods

the required thermal status of the upper composite is maintained due to the thermal inertia of the thermal cover, the fairing and the upper composite itself as well as due to the heat resistance of both the thermal cover and the fairing internal thermal blanket. This will be verified by thermal analyses carried out for each phase of ground processing.

### 5.2.3 In-flight Temperature under the Fairing

The payload fairing protects the payload during the ascent to a nominal altitude of about 120 km.

The in-flight adapter hardware temperature lies within the range  $-50^{\circ}\text{C}$  to  $+40^{\circ}\text{C}$  range without considering the payload-induced environment. During the ascent, the net flux density radiated by the fairing does not exceed  $500\text{ W/m}^2$  at any point.

Since the upper stage employs an internal temperature control system to keep the temperature of the equipment bay that directly interfaces the payload below  $50^{\circ}\text{C}$ , no induced heat load from here is to be expected. After the fairing has been jettisoned, the payload is exposed to the Free Molecular Heating (FMH) flux (section 5.2.5), solar radiation and terrestrial infrared.

#### **5.2.4 Aerothermal Flux at Fairing Jettisoning**

The time for jettisoning the fairing is determined to ensure that the aero-thermal flux of  $1135\text{ W/m}^2$  will not be exceeded. This flux is calculated as free molecular heating acting on a plane surface perpendicular to the velocity direction.

#### **5.2.5 Heat Impact during Coasting Phase**

After the fairing has been jettisoned, the spacecraft is exposed to solar radiation

flux, terrestrial albedo and terrestrial infrared radiation. The nominal orientation of the upper composite during the coasting phase is described in chapter 3.4. The heat impact to the spacecraft during the coasting phase is determined during the dedicated mission analysis. Within the requirements of the upper stage, the mission profile takes into account the spacecraft thermal requirements.

### **5.3 Fairing Static Pressure during the Ascent**

The payload compartment is vented during boosted flight. The payload compartment pressure and the depressurisation rate are a function of fairing design and flight trajectory. The nominal predicted pressure decrease profile for the *Rockot* payload fairing is shown in Figure 5-14. The maximum depressurisation rate will not exceed  $4\text{ kPa/s}$ . The static pressure within the fairing is measured during flight and transmitted to the ground using the on-board telemetry system.



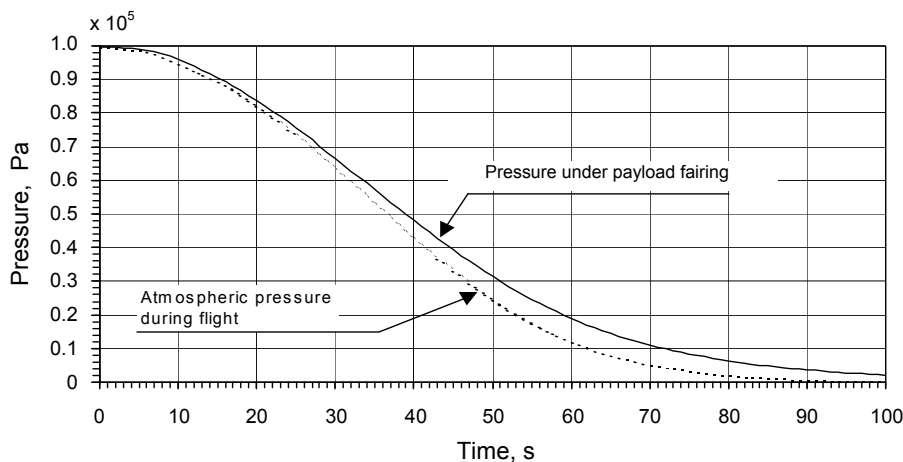


Figure 5-14 Variation of fairing inner static pressure during ascent.

## 5.4 Contamination and Cleanliness

The pyrotechnic systems used for stage, fairing and payload separation are leak proof and do not cause any organic contamination or debris. Several pyrotechnic device operations occur during the *Rocket/Breeze-KM* flight. In all cases, contamination of the spacecraft is avoided either by hermetically closed containment of the pyro charge or via the geometry of the plume relative to the payload. For payloads that are sensitive to organic contamination, a dedicated contamination analysis will be performed. The implementation of the required measures is to be negotiated and will be defined in a contamination control plan. All non-metallic materials in the upper composite are selected according to the Russian GOST standard, which specifies the use of materials with acceptable outgassing properties. ISO Standard 14644-1 Class 8 air cleanliness is provided and continuously monitored in the payload preparation rooms and inside the fairing until lift-off.

## 5.5 Electromagnetic Environment

### 5.5.1 Launch Vehicle Electro-Magnetic Emissions

The launch vehicle is equipped with the following transmission and reception systems:

- Two telemetry systems with transmitters and antennas, one in the inter-stage and one in the second stage
- A telemetry system with two transmitters and antennas in the *Breeze-KM* stage
- A transponder tracking system with a transmit-receive antenna.

During on-ground testing and during flight, the transmission systems create electric and magnetic fields. Their characteristics are presented in Table 5-14 and Figure 5-15 that define also the necessary immunity of the spacecraft against the launch vehicle and cosmodrome emissions during all operations. In all frequency portions not explicitly described in Table 5-14 the electrical field intensity is 90 dB $\mu$ V/m.

Radio transmitter	Emission frequency, MHz	Max. antenna emissive power, dBWt	Calculated level of electrical field intensity in adapter plane, dB $\mu$ V/m	
			with fairing	without fairing
Telemetry 1	120 - 130	12.3	107	119
Telemetry 2	1030 - 1050	10.0	105	117
Telemetry 3	1015 - 1025	7.8	100	112
Telemetry 4	1015 - 1025	7.8	100	112
Tracking	2700 - 3000	20.0 (pulsed mode)	107	119

**Table 5-14 Launch vehicle and cosmodrome electromagnetic emissions.**

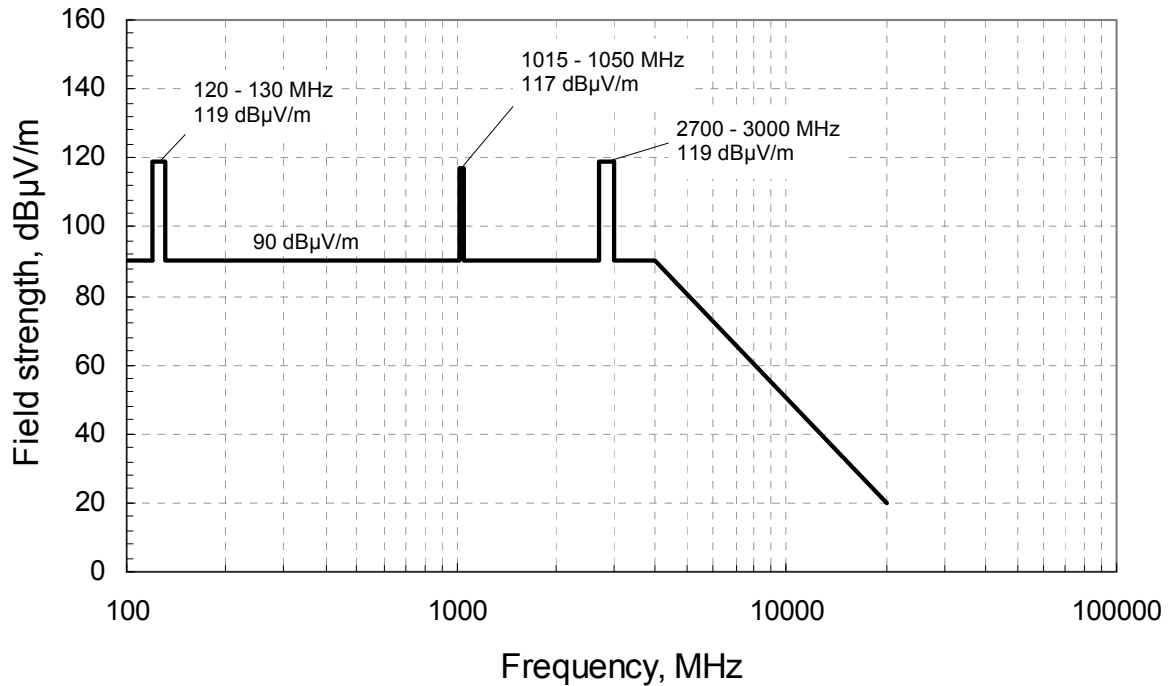


**Figure 5-15 Field strength of launch vehicle and cosmodrome electromagnetic emissions in the adapter plane without payload fairing.**

### 5.5.2 Spacecraft Electro-Magnetic Emissions

In order to avoid electromagnetic interference with the launch vehicle, the spacecraft radio frequency emission during all operations should not exceed the levels defined in Table 5-15 and Figure 5-16.

To ensure electromagnetic compatibility (EMC) between the launch vehicle and the spacecraft, a frequency plan is prepared for each launch. The Customer shall supply all data needed to support appropriate EMC analyses.

Frequency band, MHz	Allowable field strength, dB $\mu$ V/m
120 - 130	80
1015 - 1050	80
2700 - 2900	70

Table 5-15 Allowable spacecraft emissions at Plesetsk Cosmodrome.

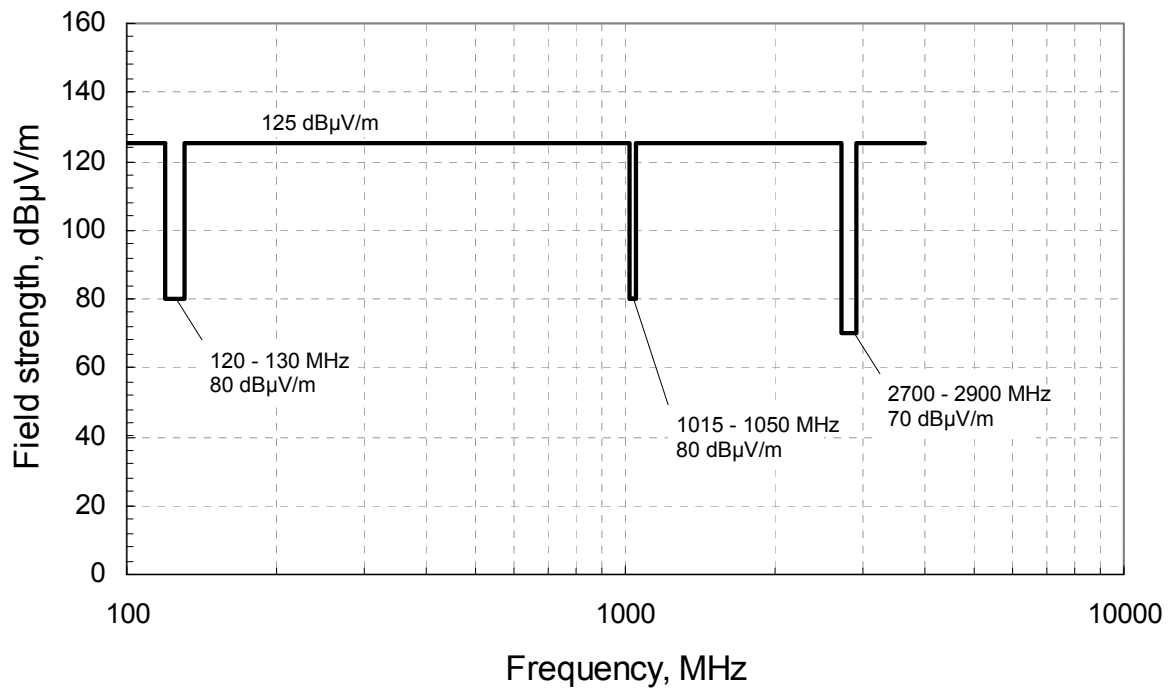


Figure 5-16 Allowable spacecraft emissions at Plesetsk Cosmodrome.

